Effects of Square-Wave Modulation on CNN Patterns

Alexander A. Alexeyev, Grigory V. Osipov, and Vladimir D. Shalfeev

Abstract—**By driving each cell (Chua's circuit) of a CNN with a nonuniform square-wave current source, different patterns are observed and reported in this paper. The dynamics of such a modulation signal could find useful applications in controlling certain features in the patterns.**

I. Introduction

IN THIS paper, we consider cellular nonlinear network (CNN) [1], [2] in which Chua's circuits are used as cells. Both an individual Chua's circuit [3] and a CNN of Chua's circuits [4]–[6] exhibit complicated dynamics. We restrict our consideration here only to structure formation that is highly interesting for theory and applications. We will focus on the effect of the modulation current source connected across the Chua's diode of each cell, as well as the coupling coefficients, on the structures of the resulting patterns.

II. Basic Model

The CNN of Chua's circuits to be studied in this paper is described by the equations [4], [5]

$$\begin{aligned}\dot{x}_j &= \alpha(y_j - h(x_j)) - \gamma_j + d_1 x_{j-1} + d_2 x_{j+1}\\ \dot{y}_j &= x_j - y_j + z_j\\ \dot{z}_j &= -\beta y_j,\\ h(x_j) &= c_1 x - \frac{2c_0 x}{1+(c_0 x)^2}, \qquad j = 1,2,\cdots,N \end{aligned} \tag{1}$$

with boundary conditions $x_0(t) = x_{N+1}(t) = 0$. The parameter γ_j is a dimensionless current corresponding to the additional current source at the jth cell [3]. The other notations are defined in [4] and [5].

The dynamics of a single cell of (1) (phase portraits and the corresponding partitioning of the (α, β) parameter plane) in the absence of coupling ($d_1 = d_2 = 0$) and current sources ($\gamma_j = 0$) are summarized in [4]. We will here consider the simplest dynamics of Chua's circuits, i.e., the case when only two stable equilibrium states $O^-(x = -a, y = 0, z = +a)$ and $O^+(x = +a, y = 0, z = -a)$ ($a = \sqrt{(2c_0 - c_1)/(c_0^2 c_1)}$) exist in the phase space. To this end, we introduce into (1) $\alpha = 1$ and $\beta = 20$, i.e., the values inside the parameter region on the (α, β) plane for which there exist two stable equilibrium states [4]. Then, for the coupling coefficients $d_1, d_2 \neq 0$, the corresponding CNN is a typical discrete *bistable* medium in which different structures may be formed. These structures consist of cells having states close to O^+ (they will further be referred to as "+" states) or close to O^- (further referred to as "−" states). We will focus attention on the formation and control of such structures by varying the parameters γ, d_1 and d_2. We will present and analyze the results of our computer experiments on (1).

Manuscript received December 16, 1994; revised April 25, 1995. This work was supported in part by the Russian Foundation for Basic Research (Grant N 93-02-15424) and by the International Association for the Promotion of Cooperation With Scientists from the Independent States of the Former Soviet Union (Grant INTAS-94-2899). This paper was recommended by Guest Editor L. O. Chua.

The authors are with Nizhny Novgorod University, Nizhny Novgorod 603600, Russia.

IEEE Log Number 9414465.

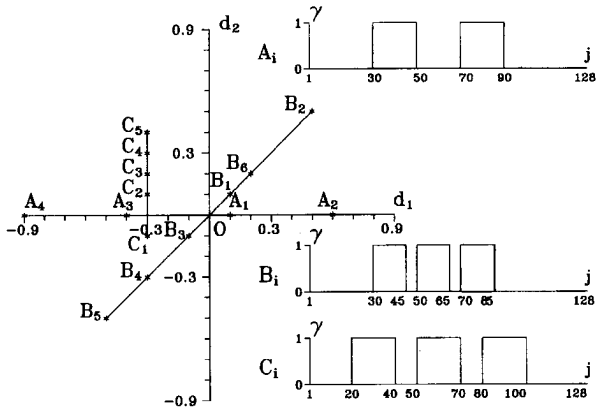

Fig. 1. The plane of coupling coefficients between the cells. The distributions of the parameter γ along the chain for which numerical experiments were performed.

III. The Formation of Structures

Consider first a 1-D CNN. Fig. 1 presents the plane of coupling coefficients (d_1, d_2) between the cells. The solid points mark the values of the parameters (on the lines A, B and C) for which numerical experiments were performed on (1).

Uniform chain ($\gamma_j = 0$)*:* In this case, (1) is symmetric relative to the coordinate origin. Therefore, the initial conditions in our computer experiments are chosen to be slightly different from zero, namely $x_j(0) = 0.1, y_j(0) = 0$ and $z_j(0) = 0.1$. The space–time diagrams of $x_j(t)$ depicting the dynamical processes in the chain (1) are given in Fig. 2(a) and (b) for the values of coupling $d_1, d_2 > 0$ (point B_2 in Fig. 1) and $d_1, d_2 < 0$ (point B_3 in Fig. 1), respectively. Time t is labeled along the horizontal scale, and the number of the cell in the chain (spatial coordinate j) is labeled along the vertical scale. The color black corresponds to the maximal value of $x_j(t)$ and white to its minimal value. It follows from Fig. 2(a) that for $d_1, d_2 > 0$ nearly all of the cells in the chain (except a few cells at the beginning and at the end of the chain) tend to the "+" state with x_j, y_j and z_j being approximately identical and equal to $x_j = x^*, y_j = y^*$, and $z_j = z^*$, where x^*, y^*, and z^* are found from the equations

$$\begin{aligned}\alpha(y^* - h(x^*)) + 2\,dx^* &= 0\\ x^* - y^* + z^* &= 0\\ y^* &= 0. \end{aligned} \tag{2}$$

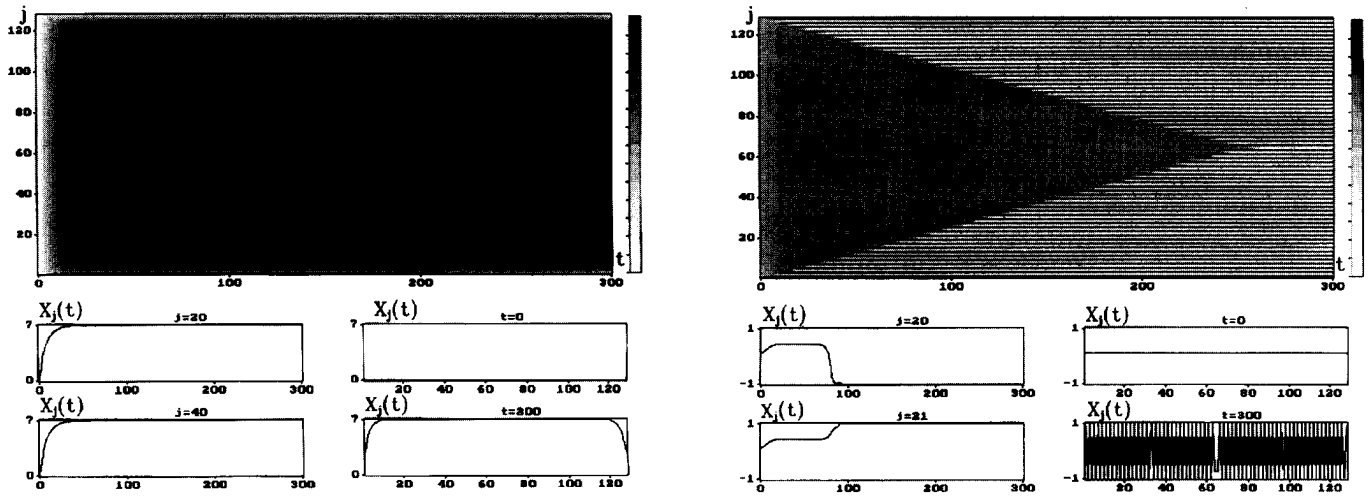

(a) (b)

Fig. 2. (a) Uniform chain ($\gamma_j = 0$). Space–time diagram of $x_j(t)$: $d_1 = d_2 = 0.5$. (Point B_2.) (b) Uniform chain ($\gamma_j = 0$). Space–time diagram of $x_j(t)$: $d_1 = d_2 = -0.1$. (Point B_3.)

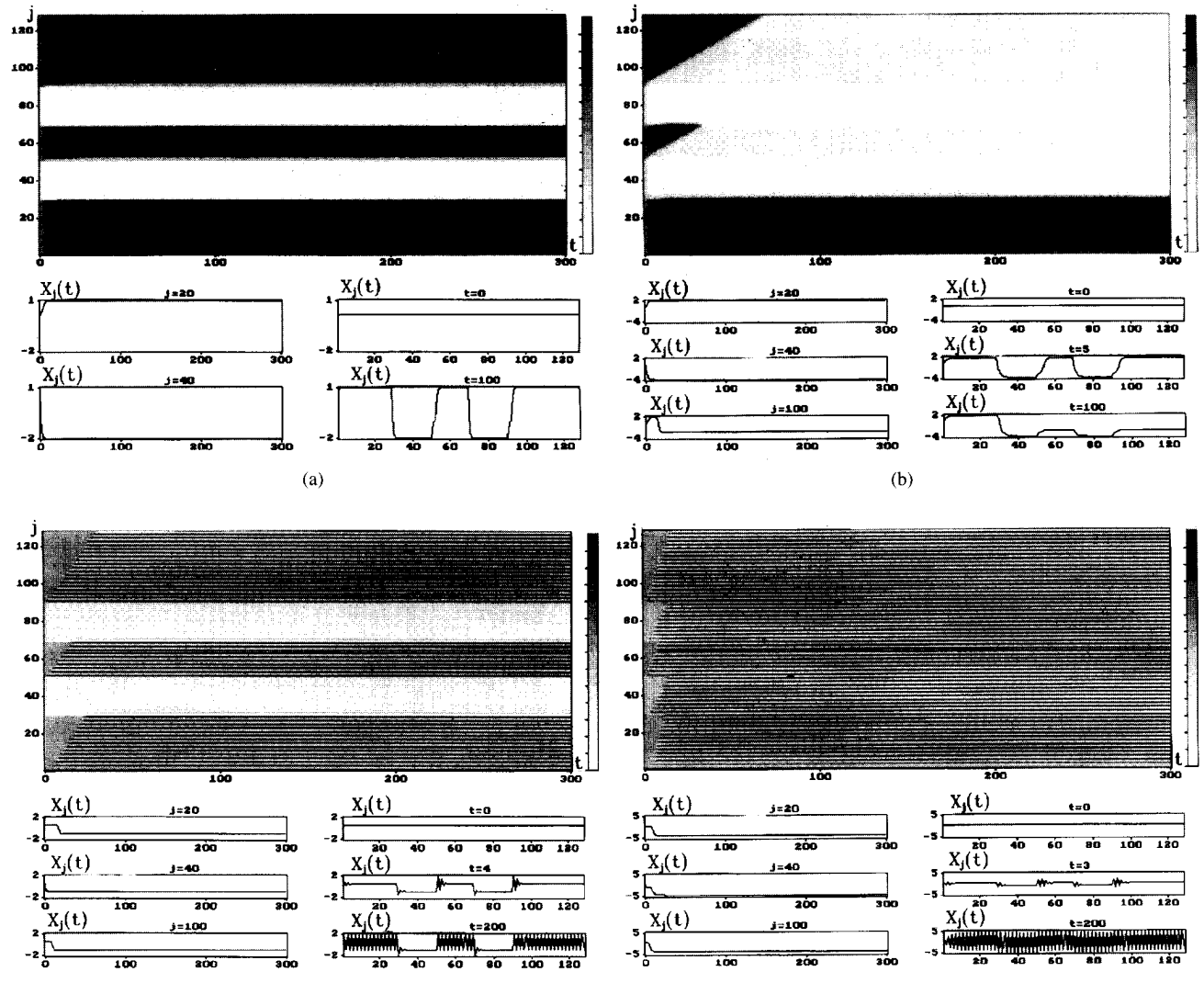

(a) (b)

(c) (d)

Fig. 3. (a) Nonuniform flow chain ($\gamma_j \neq 0, d_2 = 0$). Space–time diagram of $x_j(t)$: $d_1 = 0.1$. (Point A_1.) (b) Nonuniform flow chain ($\gamma_j \neq 0, d_2 = 0$). Space–time diagram of $x_j(t)$: $d_1 = 0.6$. (Point A_2.) (c) Nonuniform flow chain ($\gamma_j \neq 0, d_2 = 0$). Space–time diagram of $x_j(t)$: $d_1 = -0.4$. (Point A_3.) (d) Nonuniform flow chain ($\gamma_j \neq 0, d_2 = 0$). Space–time diagram of $x_j(t)$: $d_1 = -0.9$. (Point A_4.)

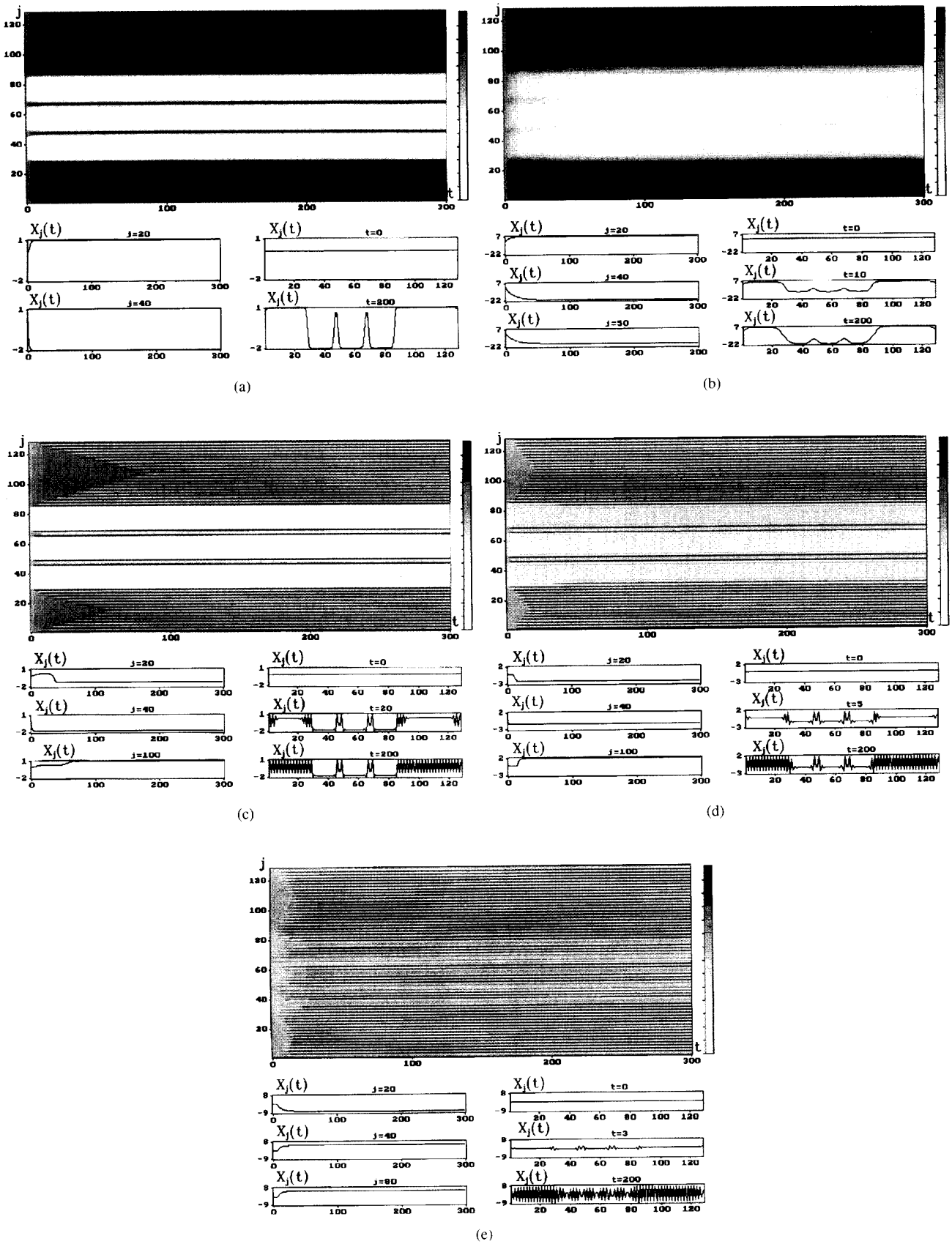

Fig. 4. (a) Nonuniform isotropic chain ($\gamma_j \neq 0, d_1 = d_2 \neq 0$). Space–time diagram of $x_j(t)$: $d_1 = d_2 = 0.1$. (Point B_1.) (b) Nonuniform isotropic chain ($\gamma_j \neq 0, d_1 = d_2 \neq 0$). Space–time diagram of $x_j(t)$: $d_1 = d_2 = 0.5$. (Point B_2.) (c) Nonuniform isotropic chain ($\gamma_j \neq 0, d_1 = d_2 \neq 0$). Space–time diagram of $x_j(t)$: $d_1 = d_2 = -0.1$. (Point B_3.) (d) Nonuniform isotropic chain ($\gamma_j \neq 0, d_1 = d_2 \neq 0$). Space–time diagram of $x_j(t)$: $d_1 = d_2 = -0.3$. (Point B_4.) (e) Nonuniform isotropic chain ($\gamma_j \neq 0, d_1 = d_2 \neq 0$). Space–time diagram of $x_j(t)$: $d_1 = d_2 = -0.5$. (Point B_5.)

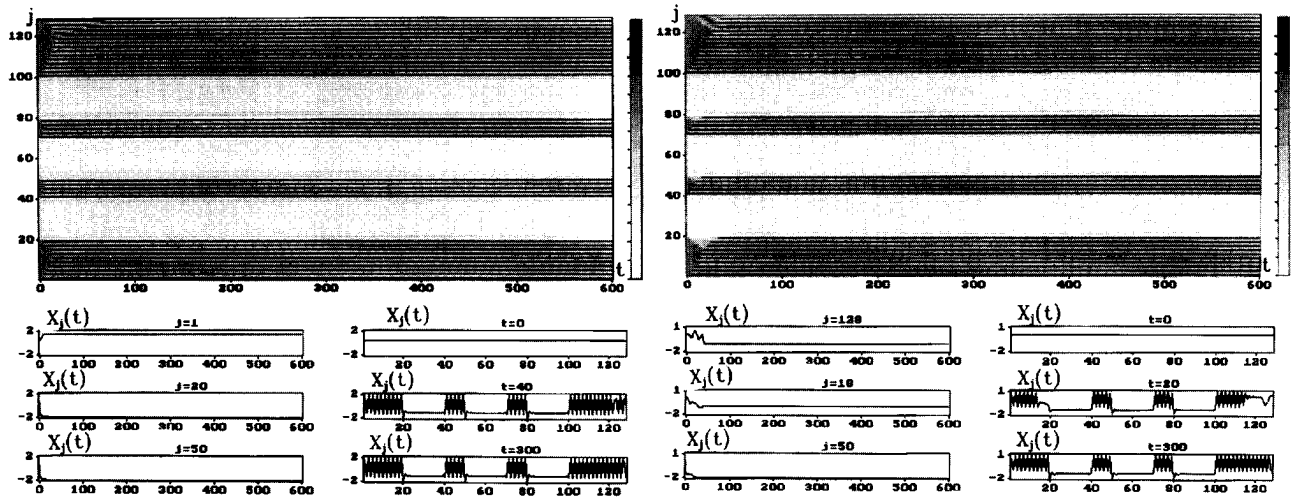

Fig. 5. (a) Nonuniform anisotropic chain ($\gamma_j \neq 0, d_1 \neq d_2$). Space–time diagram of $x_j(t)$: $d_1 = -0.3, d_2 = -0.1$. (Point C_1.) (b) Nonuniform anisotropic chain ($\gamma_j \neq 0, d_1 \neq d_2$). Space–time diagram of $x_j(t)$: $d_1 = -0.3, d_2 = 0.1$. (Point C_2.) (c) Nonuniform anisotropic chain ($\gamma_j \neq 0, d_1 \neq d_2$). Space–time diagram of $x_j(t)$: $d_1 = -0.3, d_2 = 0.2$. (Point C_3.) (d) Nonuniform anisotropic chain ($\gamma_j \neq 0, d_1 \neq d_2$). Space–time diagram of $x_j(t)$: $d_1 = -0.3, d_2 = 0.3$. (Point C_4.) (e) Nonuniform anisotropic chain ($\gamma_j \neq 0, d_1 \neq d_2$). Space–time diagram of $x_j(t)$: $d_1 = -0.3. d_2 = 0.4$. (Point C_5.)

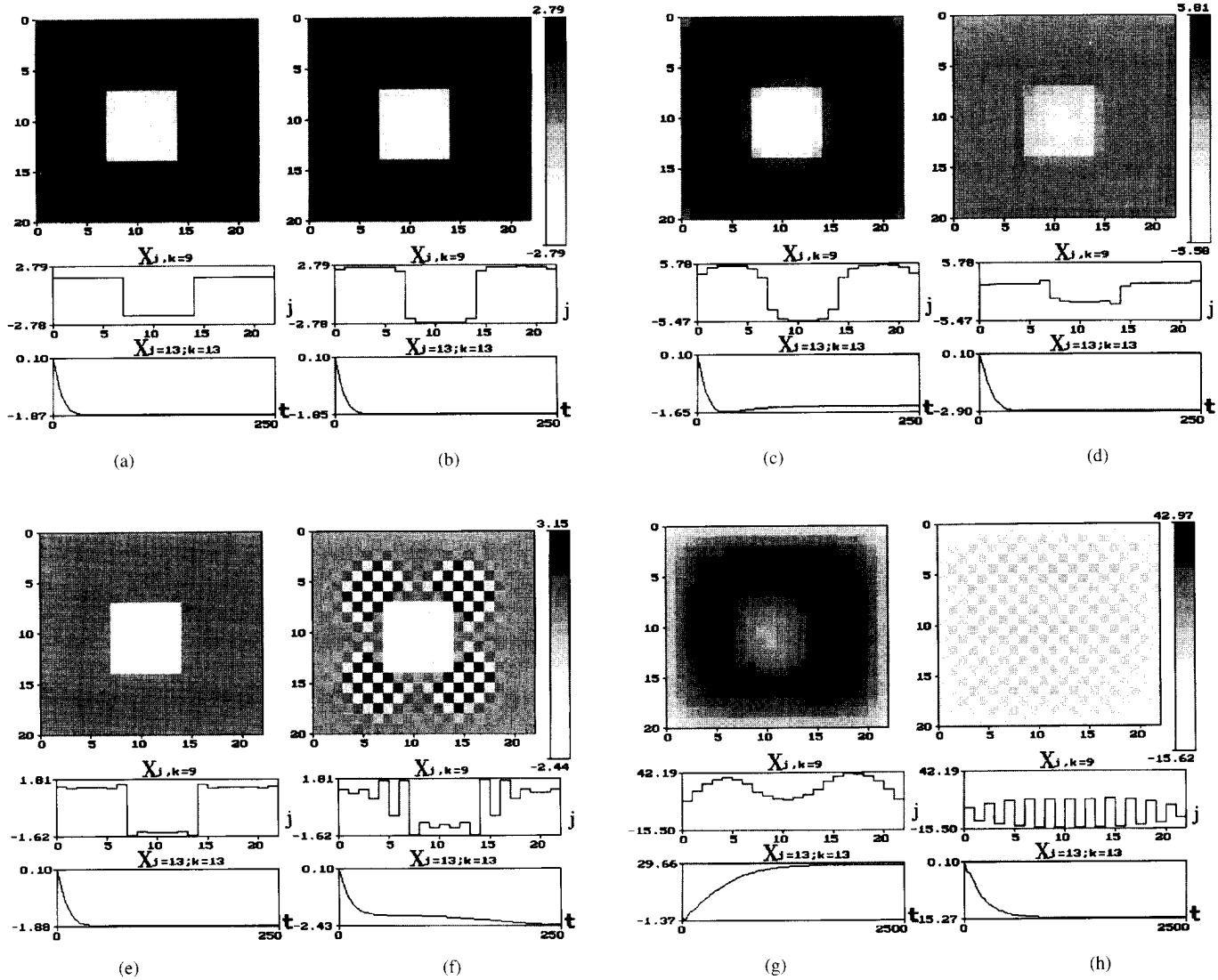

Fig. 6. 2-D CNN. Space diagram of $x_{j,k}$. (a) $d_1 = d_2 = d_3 = d_4 = 0$. (b) $d_1 = d_2 = d_3 = d_4 = 0.1$. (c) $d_1 = d_2 = d_3 = d_4 = 0.2$. (d) $d_1 = d_3 = -0.2, d_2 = d_4 = 0.2$. (e) $d_1 = d_2 = d_3 = d_4 = -0.1$. (f) $d_1 = d_2 = d_3 = d_4 = -0.2$. (g) $d_1 = d_2 = d_3 = d_4 = 0.26$. (h) $d_1 = d_2 = d_3 = d_4 = -0.26$.

For $d_1, d_2 < 0$, an oscillation *in space* between "+" and "−" states typically appear in the spatiotemporal dynamics. The transition fronts traveling from the ends of the chain towards its center where a stable spatially periodic distribution with alternating "+" and "−" states is established in the chain for $t > 250$, as shown in Fig. 2(b).

Nonuniform chain ($\gamma_j \neq 0$) : We specify a nonuniformity in the chain along γ and attempt to form in the chain "+" and "−" structures mimicking to a certain extent the nonuniformity specified along γ.

Flow (Directional) Chain ($d_2 = 0$)*:* Fig. 3(a)–(d) shows the space–time diagrams for coupling coefficients $d_1 > 0$ corresponding to points A_1, A_2, A_3, and A_4 in Fig. 1, respectively. The parameter γ is specified along the chain as follows (Fig. 1): $\gamma_j = 0$ for $j = 1, 30, 51 - 70, 91 - 128$; and $\gamma_j = 1$ for $j = 31 - 50, 71 - 90$. Our experimental results show that for sufficiently small coupling coefficients $d_1 > 0$, the stable "+" and "−" structures repeat rather well the distribution specified for γ (Fig. 3(a)). As d_1 is increased, the structures (Fig. 3(b)) become less pronounced, the process being nonsymmetric relative to the increase and decrease of j because we consider a flow (directional) chain. Structure formation occurs for small negative $d_1 < 0$ too, but instead of "+" structures, spatially periodic oscillations of "+" and "−" states are observed in Fig. 3(c). The structures become less pronounced as the coupling is increased (Fig. 3(d)).

Isotropic chain ($d_1 = d_2 \neq 0$)*:* The space–time diagrams for coupling coefficients $d_1 = d_2$ corresponding to points B_1, B_2, B_3, B_4, and B_5 in Fig. 1 are shown in Fig. 4(a)–(e). The distribution of γ is given in Fig. 1. Our experimental results confirm the regularity of formation of the structures mimicking the distribution specified along γ and, in this sense, are analogous to the previous case. The only difference is, by virtue of isotropy, that the structures become less pronounced symmetrically towards decreasing and increasing j, as the coupling coefficient is increased.

Anisotropic chain ($d_1 \neq d_2 \neq 0$)*:* The spatiotemporal dynamics in this case is illustrated in Fig. 5(a)–(e) (parameters d_1 and d_2 corresponding to points C_1–C_5 in Fig. 1). The distribution of γ is given in Fig. 1. Analogously to the previous cases, we observe formation of structures close to the specified distribution of γ as the coupling is increased. A distinguishing feature of the diagrams in Fig. 5(c)–(e) is that the processes at fixed j are periodic in time (with respect to the "+" and "−" states) and a wave of transition regimes can be observed.

2-D CNN: In this case, the equation describing the CNN has the form

$$\begin{aligned} \dot{x}_{j,k} &= \alpha(y_{j,k} - h(x_{j,k})) - \gamma_{j,k} + d_1 x_{j-1,k} \\ &\quad + d_2 x_{j+1,k} + d_3 x_{j,k-1} + d_4 x_{j,k+1} \\ \dot{y}_{j,k} &= x_{j,k} - y_{j,k} + z_{j,k} \\ \dot{z}_{j,k} &= -\beta y_{j,k} \qquad j = \overline{1,22}, \quad k = \overline{1,20}. \end{aligned} \tag{3}$$

The distribution of the "+" and "−" states in the array for zero coupling coefficients, i.e., the distribution corresponding to the specified law γ_{jk} is given in Fig. 6(a). Fig. 6(b)–(h) present the structures established in the array for different values of d_1, d_2, d_3, d_4. The structures formed in the array from "+" and "−" states, like in a 1-D CNN, mimic the original distribution $\gamma_{j,k}$ for small coupling (Fig. 6(b)–(f)). This resemblance is eventually destroyed as coupling increases (Fig. 6(g) and (h)).

IV. Conclusion

Numerical simulations of 1- and 2-D CNN of Chua's circuits have demonstrated that one can control rather effectively structure formation process by applying an external field through nonuniform square-wave current sources.

Acknowledgment

The authors wish to thank A. S. Kuznetsov for his collaboration.

References

[1] L. O. Chua and T. Roska, "The CNN paradigm," *IEEE Trans. Circuits Syst. I*, vol. 40, pp. 147–156, 1993.
[2] *Int. J. Circuit Theory and Appl.*, Special Issue on Cellular Neural Networks, vol. 20, 1993.
[3] R. N. Madan, Ed., *Chua's Circuit: A Paradigm for Chaos.* Singapore: World Scientific, 1993.
[4] G. V. Osipov and V. D. Shalfeev, "The evolution of spatio-temporal disorder in a chain of unidirectionally-coupled Chua's circuits," *IEEE Trans. Circuits Syst. I*, vol. 42, no. 10, pp. 687–692, this issue.
[5] ——, "Chaos and structures in a chain of mutually coupled Chua's circuits," *IEEE Trans. Circuits Syst. I*, vol. 42, no. 10, pp. 693–699, this issue.
[6] V. I. Nekorkin and L. O. Chua, "Spatial disorder and wave fronts in a chain of coupled Chua's circuits," *Int. J. Bifurc. and Chaos*, vol. 3, no. 5, pp. 1281–1291, 1993.

Alexander A. Alexeyev graduated from the Faculty of Radiophysics of Nizhny Novgorod State University, Russia, in 1993, in electronic engineering.

He is currently working towards the Ph.D. degree at the State University of New York at Stony Brook in the area of nonlinear dynamics of electronic systems.

Grigory V. Osipov, for a photograph and biography, see this issue, p. 692.

Vladimir D. Shalfeev, for a photograph and biography, see this issue, p. 692.